

This article was downloaded by:

On: 25 January 2011

Access details: *Access Details: Free Access*

Publisher *Taylor & Francis*

Informa Ltd Registered in England and Wales Registered Number: 1072954 Registered office: Mortimer House, 37-41 Mortimer Street, London W1T 3JH, UK



## Separation Science and Technology

Publication details, including instructions for authors and subscription information:

<http://www.informaworld.com/smpp/title~content=t713708471>

### Separation of Uranium and Plutonium from Aqueous Acidic Wastes Using a Hollow Fiber Supported Liquid Membrane

N. S. Rathore<sup>a</sup>; J. V. Sonawane<sup>a</sup>; S. K. Gupta<sup>a</sup>; Anil Kumar Pabby<sup>a</sup>; A. K. Venugopalan<sup>a</sup>; R. D. Changrani<sup>a</sup>; P. K. Dey<sup>a</sup>

<sup>a</sup> Nuclear Recycle Group, Bhabha Atomic Research Centre, Tarapur, Thane (M.S.), India

Online publication date: 08 July 2010

**To cite this Article** Rathore, N. S. , Sonawane, J. V. , Gupta, S. K. , Pabby, Anil Kumar , Venugopalan, A. K. , Changrani, R. D. and Dey, P. K.(2005) 'Separation of Uranium and Plutonium from Aqueous Acidic Wastes Using a Hollow Fiber Supported Liquid Membrane', *Separation Science and Technology*, 39: 6, 1295 – 1319

**To link to this Article:** DOI: 10.1081/SS-120030484

URL: <http://dx.doi.org/10.1081/SS-120030484>

## PLEASE SCROLL DOWN FOR ARTICLE

Full terms and conditions of use: <http://www.informaworld.com/terms-and-conditions-of-access.pdf>

This article may be used for research, teaching and private study purposes. Any substantial or systematic reproduction, re-distribution, re-selling, loan or sub-licensing, systematic supply or distribution in any form to anyone is expressly forbidden.

The publisher does not give any warranty express or implied or make any representation that the contents will be complete or accurate or up to date. The accuracy of any instructions, formulae and drug doses should be independently verified with primary sources. The publisher shall not be liable for any loss, actions, claims, proceedings, demand or costs or damages whatsoever or howsoever caused arising directly or indirectly in connection with or arising out of the use of this material.

## Separation of Uranium and Plutonium from Aqueous Acidic Wastes Using a Hollow Fiber Supported Liquid Membrane

N. S. Rathore, J. V. Sonawane, S. K. Gupta,  
Anil Kumar Pabby,\* A. K. Venugopalan,  
R. D. Changrani, and P. K. Dey

Nuclear Recycle Group, Bhabha Atomic Research Centre,  
Tarapur, Thane, India

### ABSTRACT

The use of microporous hydrophobic polypropylene, as a hollow fiber supported liquid membrane (HFSLM) was considered for removal of actinides such as uranium (U) and plutonium (Pu) from nuclear process effluents. The 1.09 M extractant, tri-*n*-butyl phosphate (TBP) diluted with *n*-dodecane was used as carrier. The study includes the hydrodynamic and chemical parameters. Modeling was performed using chemical parameters and rate controlling steps were identified. It was possible to remove U(VI) and Pu(IV) from process effluent more than 99% in presence of fission products. The optimum effective feed linear flow velocity was found to be

---

\*Correspondence: Anil Kumar Pabby, Nuclear Recycle Group, Bhabha Atomic Research Centre, Tarapur, P. O. Ghivali, Thane (M.S.) 401502, India; Fax: 91-2525-282158; E-mail: dranil@bom3.vsnl.net.in.

0.88 cm sec<sup>-1</sup>. The stripping reagent 0.1 M hydroxylamine hydrochloride (NH<sub>2</sub>OH · HCl) in 0.5 M HNO<sub>3</sub> was used. The permeation of metal ions increased with increasing effective surface area and model for higher concentration of metal ion was able to describe the transport mechanism of U(VI).

**Key Words:** HFSLM; Uranium; Flux; Extraction; Plutonium; Permeation; TBP.

## INTRODUCTION

Liquid membranes (LM) are expected to serve as one of the leading processes that will support science and technology in the near future, and continual efforts are being made to develop improved functions for membranes.<sup>[1]</sup> The partitioning of metals by LMs was actively investigated for their applications in hydrometallurgy by Li et al.<sup>[2]</sup> It is interesting to note that future trends of LM techniques are quite encouraging as these techniques continue to command significant attention, as indicated in recently published review by Sastre et al.<sup>[3]</sup>

Of late, LM processes have been suggested as a clean technology due to certain unique characteristics such as high specificity, identity, and productivity as well as low emissions and energy requirement. Several characteristics have been described by Pickering and Southern<sup>[4]</sup> in order to justify their effectiveness to be claimed as clean technology. Keeping in view of its "clean technology concept" LMs are continuously modified for their better performance in terms of stability and efficient metal transport. Membrane technology offers outstanding future potential in the reduction and/or recycling of hazardous pollutants from waste streams.<sup>[5]</sup> In contrast to distillation and solvent extraction, membrane separation is achieved normally without any phase change and use of expensive solvents.

The hollow fiber supported liquid membrane (HFSLM) module is a bundle of small porous hollow fibers randomly packed into a shell, similar in configuration to a shell and tube heat exchanger. This would allow, on one hand, the volume and the radiotoxicity of the wastes to be reduced, and, on the other hand, part of these decontaminated wastes to be directed to further treatment or disposal. The basic principle of HFSLM is the immobilization of organic extractant into the pores of hydrophobic membranes using the wetting characteristics of the membrane.<sup>[6]</sup> The main advantages of this method are: no entrainment, no flooding, very large interfacial area, the possibility to realize extreme phase ratios, independency of phase densities and interfacial tension. Hollow fiber polymeric supports are more effective because of their favorable ratio of membrane area to process volume of circulating solutions.<sup>[3,7,8]</sup>

A short-coming of HFSLM extraction could be the clogging of hollow fiber membrane pores with the suspended particles present in the feed,



which could be avoided by passing the feed solution through shell side and stripping solution through tube side. Several works exploring this technique for the extraction of metal ions,<sup>[9,10]</sup> have been published in the past decade.

These works show that the feasibility of HFSLM and its application will continue to grow in coming years. Prompted by these considerations a comprehensive program was initiated for recovery/concentration of uranium (U) and plutonium (Pu) from process effluents. Pu(IV) was taken as a representative metal ion for optimizing some important hydrodynamic parameters such as stagnant and dynamic state of strip solution, effective surface area, and membrane stability. Furthermore, U(VI) was specially taken for evaluating the diffusional parameters as it is present in higher concentration in the process effluent.

## EXPERIMENTAL

### Solvent

The organic membrane phase was prepared by dissolving a measured volume of tri-*n*-butyl phosphate (TBP) in dodecane to provide carrier solutions of varying concentrations. TBP was supplied by Shell Chemicals, Australia and analytical grade diluent, *n*-dodocane was obtained and used as such. The composition of waste solution is given in Table 1.

### Uranyl Nitrate Stock Solution

Uranyl nitrate stock solution (100 g dm<sup>-3</sup>) was prepared by dissolving U<sub>3</sub>O<sub>8</sub> powder in 1:1 nitric acid and standardized by a modified Daveis and Gray method using potentiometric end point detection.<sup>[11]</sup> From this stock solution, standard uranyl nitrate solutions of strength 15 mg cm<sup>-3</sup> in different molarity of nitric acid solutions were prepared as follows. A required aliquot of uranyl nitrate stock solution was pipetted in a ground glass-stoppered tube

**Table 1.** Composition of simulated medium active aqueous acidic waste.

Uranium	15 g dm <sup>-3</sup>
Plutonium	8 mg dm <sup>-3</sup>
Gross $\beta$	49.3 mCi dm <sup>-3</sup>
Gross $\gamma$	15.7 mCi dm <sup>-3</sup>
Acidity	3 M HNO <sub>3</sub>



and evaporated to dryness under infra-red lamp in a fume hood. The residue was dissolved subsequently in the required volume of particular desired strength of nitric acid solution.

### Tracers

Tracers such as  $^{233}\text{U}$ ,  $^{239}\text{Pu}$ ,  $^{137}\text{Cs}$ ,  $^{106}\text{Ru}$ , and  $^{154,152}\text{Eu}$ , were obtained from Isotope Division, BARC, Mumbai. Whenever required, the desired tracers were evaporated to dryness and made up with required molarity of nitric acid solution used for experiments.

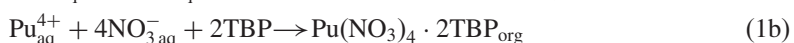
Uranium estimation is carried out using alcoholic ammonium thiocyanate method.<sup>[12]</sup> This method is well suited for the estimation of U(VI) in the range of 0.1–5.0 mg in  $25\text{ cm}^3$  final volume. The molar absorptivity of  $1000\text{ L mol}^{-1}\text{ cm}^{-1}$  at 420 nm and  $5000\text{ L mol}^{-1}\text{ cm}^{-1}$  at 375 nm, makes the method quite sensitive.

### Alpha Scintillation Counting

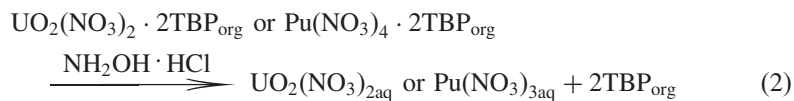
For  $^{233}\text{U}$  and  $^{239}\text{Pu}$ , PLA make alpha scintillation counter with ZnS(Ag) as a detector was used to determine the concentration of these alpha emitting actinides in the aqueous phase by radiometry. The total alpha in the sample was estimated by direct planchetting on a 2.5 cm diameter stainless steel planchet and counting on alpha scintillation counter. Every time efficiency of the counter was checked by comparing it with standard alpha source and background was checked and proper correction was incorporated in calculations of activity. Plutonium alpha activities were determined by extracting plutonium in 0.5 M theonyltrifluoro acetone (TTA)/xylene and directly planchetting the organic phase. Alpha spectrometry of the planchets was done using a silicon surface-barrier detector to detect the presence of Pu.

### Mechanism of U(VI)/Pu(IV) Transport

When the  $\text{UO}_2^{2+}/\text{Pu}^{4+}$  ions in the feed side come in contact with TBP in the LM in the presence of  $\text{H}^+$  and  $\text{NO}_3^-$  ions (in the source phase) the following reactions takes place<sup>[13,14]</sup>



As the  $\text{UO}_2(\text{NO}_3)_2 \cdot 2\text{TBP}_{\text{org}}$  or  $\text{Pu}(\text{NO}_3)_4 \cdot 2\text{TBP}_{\text{org}}$  complex is formed on the membrane interface on the feed side, its concentration within the membrane on this side increases. Subsequently, it moves towards the stripping solution within the membrane as a consequence of concentration gradient. As the complex reaches the product side of the membrane, the following reaction takes place



The TBP molecules are left free in the organic membrane phase and the  $\text{UO}_2(\text{NO}_3)_2/\text{Pu}(\text{NO}_3)_3$  species enters the product side. The concentration of the  $\text{UO}_2(\text{NO}_3)_2 \cdot 2\text{TBP}$  or  $\text{Pu}(\text{NO}_3)_4 \cdot 2\text{TBP}$  neutral complexes in the LM remains high on the source phase side because the complexes are continuously being formed in that side and their concentration remains very low on the product side as distribution ratios (*D* values) of actinides are very low with stripping reagent. Consequently, the complexes go on permeating continuously from the feed to the product side across the LM under its concentration gradient. As  $\text{NO}_3^-$  ions moves in the direction of  $\text{UO}_2^{2+}/\text{Pu}^{4+}$  ions, there is a coupled co-transport process. At high  $\text{HNO}_3$  concentrations, the  $\text{TBP} \cdot \text{HNO}_3$  type complex is also formed, which competes with metal-ligand complex transport and results in decline the overall transport process.

### Characteristics of the Membrane and Device

Supports for the HFSLM, were obtained from ENKA (Germany). The morphology of the lumens is depicted in elsewhere.<sup>[15]</sup>

Hydrophobic polypropylene hollow fibers having following specification were used to fabricate the modules:

Material	Polypropylene	Fiber I.D. (mm)	0.6
Porosity (%)	70	Shape	Tubular
Effective pore size ( $\mu\text{m}$ )	0.2	Module structure	Shell and tube
Fiber wall thickness ( $\mu\text{m}$ )	200	Surface area ( <i>A</i> ) ( $\text{cm}^2$ )	$\sim 34$
Fiber length (cm)	9.0	Module length (cm)	10
Fiber O.D. (mm)	1.0	Module diameter (cm)	1.0



### Permeation Study

The hollow-fiber module was operated in a recirculating mode. The feed and strip solutions were circulated through the lumen and on the shell side of fibers, respectively, by means of calibrated peristaltic pump. The permeation of the radionuclides through the HFSLM was examined periodically by sampling the feed and/or strip solution. Sample was analyzed for  $\alpha$  using ZnS silver activated scintillation counter and for  $\gamma$  using NaI (Tl) scintillation counter and uranium by spectrophotometry.

## RESULTS AND DISCUSSION

### Extraction Equilibrium for Uranium

The  $\text{UO}_2^{2+}$  ion in nitrate medium ( $\text{HNO}_3$ ) form  $\text{UO}_2(\text{NO}_3)_2 \cdot 2\text{TBP}$  complex with the extractant, expressed as Eq. (1)<sup>[13]</sup> and stripping of U(VI) from loaded TBP is as Eq. (2), the extraction equilibrium can be described by the following equation and extraction constants for U:

From Eq. (1a)

$$K_{\text{ex}} = \frac{[\text{UO}_2(\text{NO}_3)_2 \cdot 2\text{TBP}]_{\text{org}}}{[\text{UO}_2^{2+}]_{\text{aq}} [\text{NO}_3^-]_{\text{aq}}^2 [\text{TBP}]_{\text{org}}^2} \quad (3)$$

$$D_U = \frac{[\text{UO}_2(\text{NO}_3)_2 \cdot 2\text{TBP}]_{\text{org}}}{[\text{UO}_2^{2+}]_{\text{aq}}}$$

or

$$K_{\text{ex}} = \frac{D_U}{[\text{NO}_3^-]_{\text{aq}}^2 [\text{TBP}]_{\text{org}}^2}$$

The values of  $K_{\text{ex}}$  for U(VI) with TBP in dodecane were calculated from the  $D_U$  values. The partition coefficient could be presented as

$$\log D_U = \log K_{\text{ex}} + 2 \log [\text{NO}_3^-] + 2 \log [\text{TBP}]_{\text{org}} \quad (4a)$$

Similarly for Pu extraction equilibria can be presented as:

$$\log D_{\text{Pu}} = \log K_{\text{ex}} + 4 \log [\text{NO}_3^-] + 2 \log [\text{TBP}]_{\text{org}} \quad (4b)$$

Permeation of U(VI) and Pu(IV) have been studied with hollow-fiber membrane supports assembled in laboratory-scale modules. Detailed investigations



were undertaken to define the best operating conditions and to consider how selectivity and durability of operation could be ensured. As a representative case, Pu(IV) was selected and experiments were conducted for the operation of HFSLM, in varying parameters such as flow rate, surface area, carrier concentration, nitrate ion concentration, circulation of the feed/strip solution from different geometry and recirculation rate of strip solution etc.

### Effect of Carrier Concentration on the Permeability Coefficient

The composition of the organic solution has a significant effect on the permeation when transport across a membrane occurs via a carrier, the permeability is expected to increase with increase in carrier concentration. However, in carrier-mediated transport of Pu with TBP, a more complex behavior is seen.<sup>[15]</sup> Table 2 summarizes data for uranium flux vs. TBP concentration in the membrane. It is obvious that similar behavior as with Pu was observed in case of uranium. Reusch and Cussler<sup>[16]</sup> have also shown that the diffusion limited flux linearly increases with the carrier concentration; but at higher carrier concentration the viscosity of the membrane phase also increases. The increase in membrane viscosity has often led to an optimum in the flux as a function of the carrier concentration. This interesting phenomenon is apparently caused by two competing factors:

- The concentration gradient of the uranium/plutonium complex.
- The viscosity of the carrier/diluent in the LM.

**Table 2.** Effect of carrier concentration on the flux of uranium transport across HFSLM.

Experiment no.	Concentration of TBP (M)	Flux <sup>a</sup> ( $10^{-11}$ )	Permeability coefficient <sup>b</sup> ( $10^{-7}$ )
1	0.36	3.26	1.12
2	0.72	4.83	1.67
3	1.09	4.66	1.61
4	1.45	1.54	0.53
5	1.81	1.18	0.48

*Note:* Feed,  $U^{233}$  tracer; feed and stripping volume ratio, 1; acidity, 3 M  $HNO_3$ ; flow rate for HFSLM,  $2.5 \text{ mL min}^{-1}$ ; surface area,  $33.9 \text{ cm}^2$  (HFSLM); strippant, 0.1 M  $NH_2OH \cdot HCl$  in 0.3 M  $HNO_3$ .

<sup>a</sup>Flux  $J$  ( $\text{mol cm}^{-2} \text{ sec}^{-1}$ ) = permeability coefficient ( $P_U$ )  $\times C$  (concentration of U).

<sup>b</sup> $P_U$ ,  $\text{cm sec}^{-1}$ .



As the diffusion coefficient ( $D$ ) of a solute, across the membrane is defined by the following Stokes–Einstein equation:

$$D = \frac{kT}{6\pi r\eta} \quad (5)$$

where  $k$ ,  $T$ ,  $r$ , and  $\eta$  denote the Boltzmann constant, the absolute temperature, the molecular radius of the metal-complex and the viscosity of the organic phase, respectively.

Since flux is inversely proportional to the viscosity, an increase in the viscosity should reduce the transport which has been confirmed by increasing in viscosity by taking higher concentration of carrier. Thus 30% TBP was selected as the optimum carrier concentration to carry out further experiments to standardize different operating parameters.

#### Effect of Strip Solution with Agitated and Stagnant State

Experiments were carried out with strip solution in recirculating mode [1] and without recirculating mode [2]. For the mode [1], both feed solution and striping solution are recycled, whereas in case of mode [2] feed solution is recycled and strip solution kept stagnant. Table 3 shows the results from both the experiments. The recirculating mode gave more permeation ( $\sim 81.5\%$ ) than the stagnant mode (59.9%). Effective agitation of strip aqueous phase, decreases the thickness of aqueous strippant boundary layer's ( $d_a$ ). Therefore, instantaneous contact of fresh strippant with membrane takes place thus fast stripping of metal ion from loaded organic at the membrane–strip inter phase was observed.

The performance of various contactor configurations have been reported for parallel and transverse flow across the fiber to compare the efficiency that can be obtained in commercially-made modules.<sup>[17]</sup> It is found in a number of studies that fluid flow outside fibers shows major channeling causing a reduction in the mass transfer coefficients. More recently, Lipnizki and Field<sup>[18]</sup> categorizes general effects on mass transfer during shell-side flow at different packing fractions. At low packing densities, maldistribution competes with transverse flow and other effects while at high packing fractions, channeling and dead zones in the modules are major effects. Very accurate specific correlations can be developed for shell-side flow; it is often based on experiments on particular types of module and may be limited in the range of packing densities where it is being applied.

In HFSLM, with circulation of feed solution through shell side and strip solution through tube side, transport of Pu was significantly varied. As the feed solution flowed through the shell side, part of the flowing solution escaped without contact of the membrane phase, which resulted in poor performance of



**Table 3.** Permeation percentage of plutonium with different flow state of strip solution.

Time (min)	Percentage permeation (%P)	
	Stagnant state	Dynamic state
8	7.6	21.5
16	19.8	34.0
24	29.4	47.4
32	30.3	48.5
40	33.9	50.7
48	37.3	56.9
56	46.8	62.6
64	48.7	78.4
72	54.6	80.1
80	59.9	81.5

*Note:* Feed, plutonium nitrate solution; feed and strip ratio, 1; acidity, 3 M HNO<sub>3</sub>; flow rate for feed and strip, 2.5 mL min<sup>-1</sup> (in case of dynamic state); surface area, 33.9 cm<sup>2</sup> (HFSLM); strippant, 0.1 M NH<sub>2</sub>OH · HCl in 0.3 M HNO<sub>3</sub>; carrier concentration, 1.09 M (~30%) TBP in *n*-dodecane.

the HFSLM compared to the feed flowing through the lumens. The model is explained in Fig. 1(A). The results from Fig. 1(B) indicated that the percentage permeation obtained by feed flowing through the shell side was 47%, which is lesser than the percentage permeation 82%, when feed was flowing through tube side. The percentage permeation (%P) was almost half of that obtained by the flowing feed tube side and stripping solution shell side. Probably reduction in overall %P results due to the lowering of linear flow velocity of the feed solution when the solution passed through the shell side.<sup>[8]</sup> Another reason for the decrease in Pu permeability was probably the insufficient membrane area provided for the stripping reaction in the tube side as compared to the shell side. Therefore, the mode (feed flowing through the tube side) operation was adopted through in order to obtain a more transport.

### HFSLM Cation Selectivities

Selective tributyl phosphate-mediated cation transport using HFSLM was also investigated as has been done in flat-sheet supported LM systems. This is to demonstrate the selectivity of the uranium and plutonium in order to examine the effect of several other metal ions generally accompanying



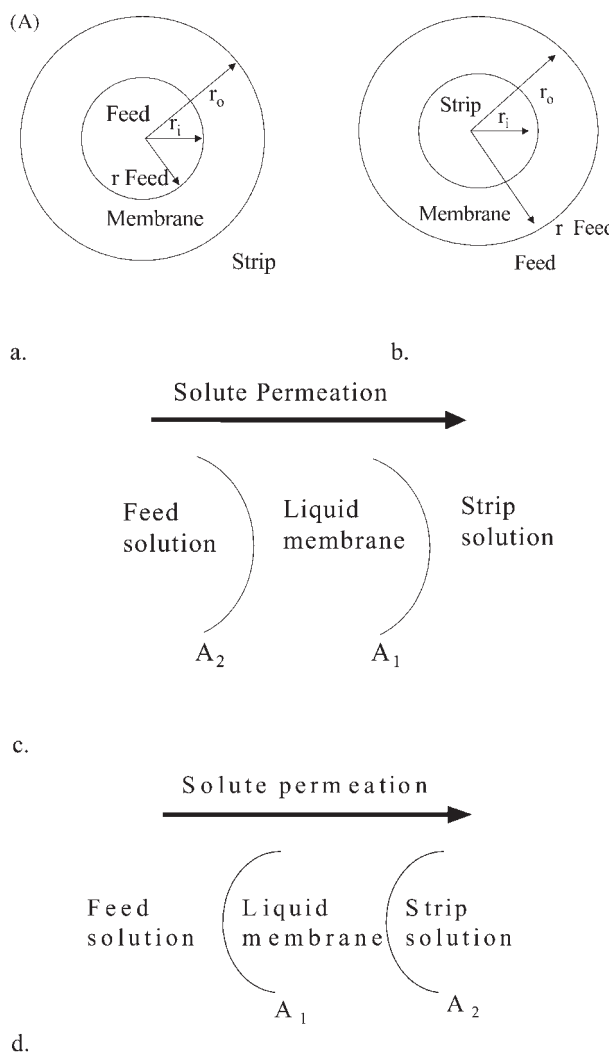


**Figure 1.** (A) Cross-section of hollow fiber with characterizing sizes. (a) Feed on tube side; (b) feed on shell side; (c) and (d) HFSLM configuration:  $A_1$  and  $A_2$  are the inner and outer surface areas of the support membrane, respectively.  $r_i$ , inner radius;  $r_o$ , outer radius. (B) Percentage permeation (%) of Pu(IV) for two different feed recirculating condition. Acidity: 3 M  $HNO_3$ ; carrier: 1.09 M TBP in dodecane; strip:  $NH_2OH \cdot HCl$  in 0.3 M  $HNO_3$ ; feed linear flow velocity:  $0.88 \text{ cm sec}^{-1}$ .



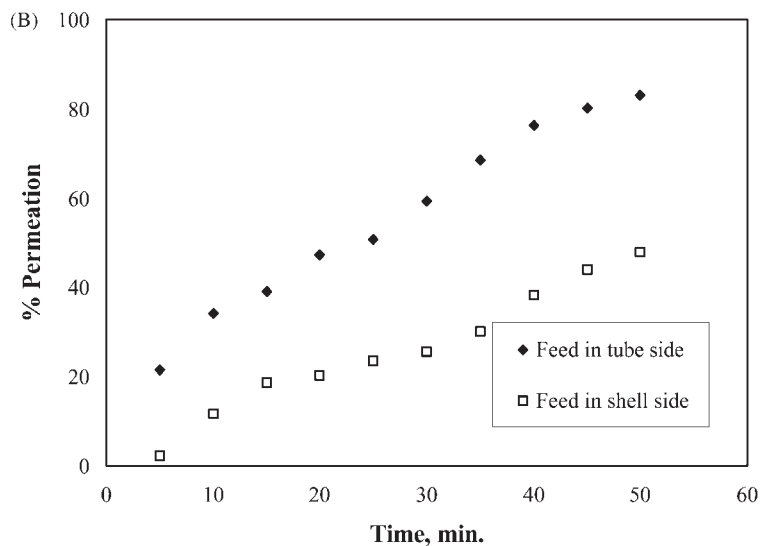


Figure 1. Continued.

$\text{Pu}(\text{NO}_3)_4/\text{UO}_2(\text{NO}_3)_2$  and their interferences with overall permeation of  $\text{Pu}(\text{IV})/\text{U}(\text{VI})$ . In aqueous acidic wastes solutions there are hosts of nitrate ions that can be found. Cation selectivity measurements were obtained with HFSLM using 1.09 M ( $\sim 30\%$  TBP v/v) TBP in dodecane as the LM for various metal nitrate like, cesium ( $^{137}\text{Cs}$ ), ruthenium ( $^{106}\text{Ru}$ ), and europium ( $^{154}\text{Eu}$ ). The conditions were similar to those encountered in radiochemical waste solutions from nuclear chemical facilities. Fig. 2 presents the results of  $\text{U}(\text{VI})$  and  $\text{Pu}(\text{IV})$  permeability, in presence of these fission products like  $^{137}\text{Cs}$ ,  $^{106}\text{Ru}$ , and  $^{154}\text{Eu}$ , was not affected as there was no transport of Cs, Ru, and Eu. This may be due to negligible distribution coefficient and high separation factor (SF) which is defined as

$$\text{SF}_M = \frac{P_M}{P_m} \quad (6)$$

where  $P$  = permeability coefficient,  $M = \text{U}$  and  $\text{Pu}$ ,  $m$  = fission products in TBP/*n*-dodecane system for such fission products.

#### Surface Area Variation

To study the influence of the variation of the surface area ( $A$ ), permeability coefficients ( $P_{\text{Pu}}$ ) were determined using three different



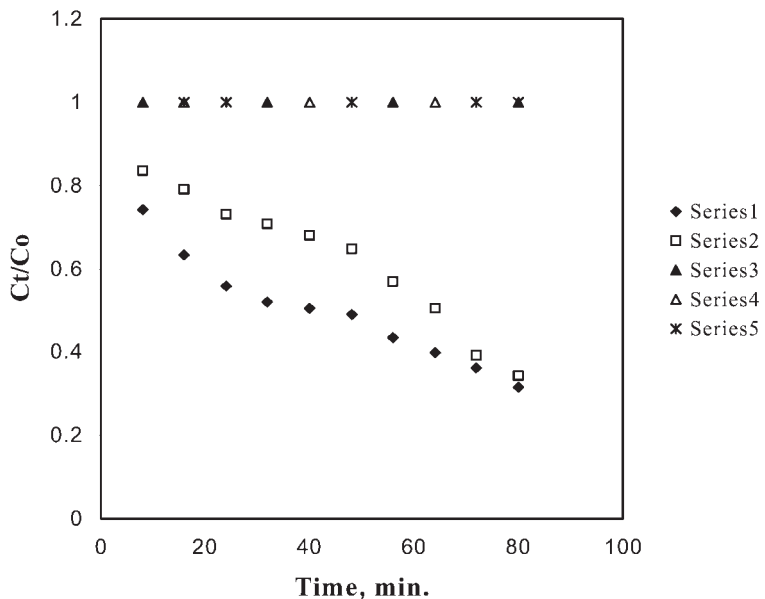


**Figure 2.** Effect of other metal nitrate ions such as Cs-137, Ru-106, and Eu-154, on U(VI) and Pu(IV) permeation. Carrier concentration: 1.09 M TBP; stripping phase: 0.1 M  $\text{NH}_2\text{OH}\cdot\text{HCl}$  in 0.3 M  $\text{HNO}_3$ ; flow rate: 3  $\text{mL min}^{-1}$ ; feed acidity: 3 M  $\text{HNO}_3$ . Series 1, uranium; Series 2, Pu; Series 3 ruthenium; Series 4, europium; Series 5, caesium.

cell modules containing varying number of lumens and  $P_{\text{Pu}}$  was calculated using points from Fig. 3. The result shows that the  $P_{\text{Pu}}$  for  $8.5 \text{ cm}^2$  (five lumens) was found to be  $1.2 \times 10^{-5} \text{ cm sec}^{-1}$ , surface area  $25.4 \text{ cm}^2$  (15 lumens) it was observed to be  $1.4 \times 10^{-5} \text{ cm sec}^{-1}$  and for surface area  $33.9 \text{ cm}^2$  (20 lumens) it was seen to be  $1.5 \times 10^{-5} \text{ cm sec}^{-1}$ . Studies show that modules with greater membrane area per unit volume perform better than those with smaller area per unit volume.<sup>[17]</sup>

### Influence of Initial Permeant Concentration on Permeation

The influence of metal ion concentration [ $10^{-5}$ – $10^{-4}$  M U(VI)] on permeability was studied.<sup>[19]</sup> The flux for two different concentration of metal ion was calculated from slope analysis technique with data taken from Fig. 4 and was observed to be  $3.49 \times 10^{-9} \text{ mol cm}^{-2} \text{ sec}^{-1}$  at U concentration  $2.89 \times 10^{-4} \text{ mol dm}^{-3}$  and  $1.5 \times 10^{-10} \text{ mol cm}^{-2} \text{ sec}^{-1}$  at  $1.93 \times 10^{-5} \text{ mol dm}^{-3}$  uranium concentration.



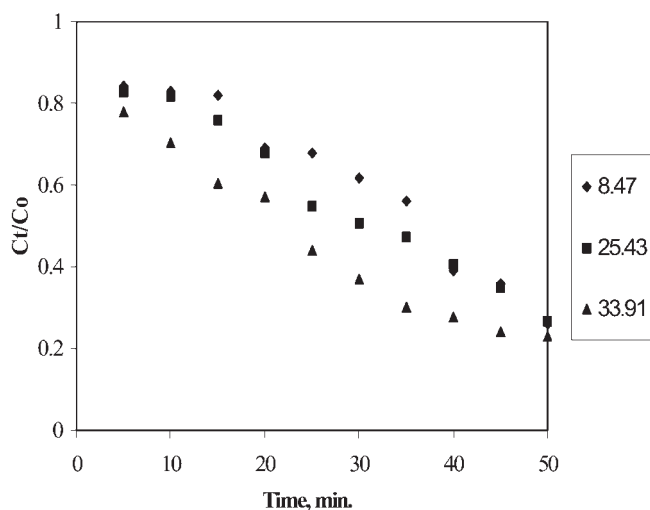


**Figure 3.** Plot of the variation of effective surface area ( $A$ ) on Pu(IV) permeation. Carrier: 1.09 M TBP in dodecane; stripping phase: 0.1 M  $\text{NH}_2\text{OH}\cdot\text{HCl}$  in 0.3 M  $\text{HNO}_3$ ; feed linear flow velocity:  $0.88 \text{ cm sec}^{-1}$ ; feed  $\text{H}^+$ : 3 M  $\text{HNO}_3$ . Series 1,  $8.47 \text{ cm}^2$ ; Series 2,  $25.43 \text{ cm}^2$ ; Series 3,  $33.91 \text{ cm}^2$ .

The higher uranium and plutonium concentration yielded higher flux, between the range  $10^{-6}$  and  $10^{-4}$  M. This may be due to higher concentration gradient between the aqueous feed phase to stripping phase across the LM, since the incomplete saturation of organic with the metal ion at this very low level of two concentration takes place. Once the concentration of metal ion further increased to sufficient saturation of the carrier, the permeability of metal ion may decrease, because at this stage,  $J$  becomes constant, probably for two reasons: firstly, membrane saturation, lower effective membrane area of the HFSLM, and secondly, maximization owing to saturation of the membrane pores with metal–carrier species and in addition, the build-up of a carrier layer on the membrane interface which assists the retention of the separating constituent on the entry side and leads to a constant permeability flux.<sup>[20]</sup> On the contrary, in our case the carrier concentration is much higher than the metal ion concentration taken for the study. Therefore, at this level of two different concentration for plutonium as well as uranium, concentration gradient for higher metal ion concentration was more which maintained the uphill transport of Pu(IV) and U(VI) ions from the feed phase to strip phase across the membrane. Thus the wastes, having concentration in these ranges are more suitable for decontamination through HFSLM module without observing significant decrease in permeability.



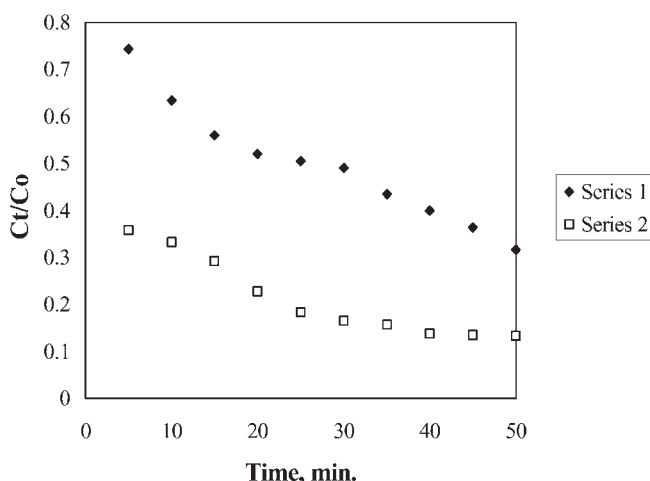


**Figure 4.** Influence of initial concentration of U(VI) on permeability flux ( $J$ ) with carrier concentration: 1.09 M TBP in dodecane; stripping agent: 0.1 M  $\text{NH}_2\text{OH} \cdot \text{HCl}$  in 0.3 M  $\text{HNO}_3$ ; feed linear flow velocity:  $0.88 \text{ cm sec}^{-1}$ ; feed  $\text{H}^+$ : 3 M  $\text{HNO}_3$ . Series 1,  $1.93 \times 10^{-5} \text{ mol dm}^{-3}$ ; Series 2,  $2.89 \times 10^{-4} \text{ mol dm}^{-3}$ .

Danesi<sup>[21]</sup> derived equation for the two limiting cases of low and high metal concentrations of the feed solutions. When the metal concentration is low, the concentration of the unbound carrier essentially equals the total membrane carrier concentration. In this case the membrane flux varies with time and along the hollow-fiber axial coordinate. The equation derived in this case only hold in a region of low product recovery.<sup>[15]</sup> As medium active wastes consists uranium in  $\text{g dm}^{-3}$  level (Table 1). Thus transport of higher concentration of metal ion in feed becomes essential part of this study. When the metal concentration is high, the concentration of the unbound carrier is close to zero and the membrane flux is constant with time and along the hollow-fiber axial coordinate. When the metal concentration in the aqueous feed is high and the membrane carrier is completely loaded with permeating metal, Eq. (5)<sup>[15]</sup> is no longer valid, hence, we should derive the equation for HFSLM system run in recycling mode as suggested by Danesi<sup>[21]</sup> and Aamrani et al.<sup>[22]</sup> We consider the chemical reaction expressed in Eq. (1a) and denote by:

$$[\text{U}]_{\text{org}} = [\text{UO}_2(\text{NO}_3)_2 \cdot 2\text{TBP}]_{\text{org}}$$

where  $[\text{U}]_{\text{org}}$  is concentration of uranium in organic phase.



Taking into account Eq. (1a) for equilibrium constant of this chemical reaction as shown below:

$$[U]_f^{\text{org}} = K_{\text{ex}} [NO_3^-]_{\text{aq}}^2 [TBP]_{\text{org}}^2 [UO_2^{++}]_f \quad (7a)$$

where  $[U]_f^{\text{org}}$  is interfacial concentration of uranium complex.

Now from Ref.<sup>[23]</sup>

$$K_{\text{ex}} = \frac{[U]_f^{\text{org}}}{[UO_2^{++}]_{\text{aq}} [NO_3^-]_{\text{aq}}^2 [TBP]^2}$$

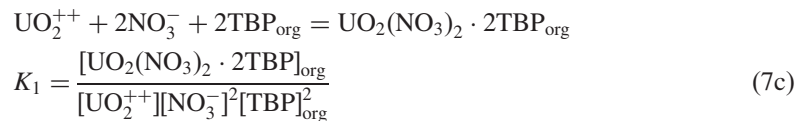
from Eq. (3) using

$$[U]_{\text{org}} = [UO_2(NO_3)_2 \cdot 2TBP]_{\text{org}}$$

Eq. (3) becomes

$$[TBP]_{\text{org}}^2 = \frac{[U]_{\text{org}}}{[UO_2^{++}] [NO_3^-]_{\text{aq}}^2 K_{\text{ex}}} \quad (7b)$$

It is derived according to Ref.<sup>[21]</sup>. The extraction equilibrium can be described for TBP [Eq. (7c)] by the reaction and extraction constants given below as:



The uranium transport rate is determined by the rate of diffusion of uranium-containing species through the feed diffusion layer and the rate of diffusion of  $UO_2(NO_3)_2 \cdot 2TBP$  through the membrane. Then, the flux of  $UO_2^{++}$  crossing the membrane may be derived by applying Fick's first diffusion law to the diffusion layer on the feed side, and to the membrane. The diffusional fluxes at the feed aqueous boundary layer  $J_{af}$  and at the membrane phase  $J_o$  for TBP [Eq. (7e)] can be expressed by the following equations, assuming that the diffusion coefficient of  $UO_2(NO_3)_2 \cdot 2TBP$  is the same in the membrane phase:

$$J_{af} = \Delta_{af}^{-1} ([U]_{\text{tot}} - [U]_{i,\text{tot}}) \quad (7d)$$

$$J_o = \Delta_o^{-1} ([UO_2(NO_3)_2 \cdot 2TBP]_{if} - [UO_2(NO_3)_2 \cdot 2TBP]_{i,is})$$

$$\Delta_a = \frac{d_a}{D_a}, \quad \Delta_o = \frac{d_o}{D_o} \quad (7e)$$

As the distribution coefficient of  $UO_2^{++}$  between the membrane phase and the stripping phase is much lower than that between the



feed phase and the membrane, the concentration of the metal-extractant complexes in the membrane phase on the stripping solution side may be negligible compared with that on the feed solution side. Then, Eq. (7e) can be written as:

$$J_o = \Delta_o^{-1} [UO_2(NO_3)_2 \cdot 2TBP]_{if} \quad (7f)$$

If the chemical reactions expressed by Eq. (7c)<sup>[15]</sup> is assumed to be fast compared to the diffusion rate, local equilibrium at the interface is reached and concentrations at the interface is related through Eq. (7c).

From Eq. (3) and (7f)

$$\begin{aligned} J_o \Delta_o &= [UO_2(NO_3)_2 \cdot 2TBP]_{if} = K_{ex}[TBP]_{org}^2 [NO_3^-]^2 [UO_2^{2+}]_{if} \quad \text{or} \\ &= \frac{J_o \Delta_o}{K_{ex}[TBP]_{org}^2 [NO_3^-]^2} = [UO_2^{2+}]_{if} \end{aligned} \quad (8a)$$

From Eq. (7d)

$$J_a \Delta_a = [UO_2^{2+}]_f - [UO_2^{2+}]_{if} \quad (8b)$$

We substitute Eq. (8a) in to Eq. (8b) to obtain  $[[UO_2^{2+}]_f]$ ,

$$J_a \Delta_a = [UO_2^{2+}]_f - \frac{J_o \Delta_o}{K_{ex}[TBP]_{org}^2 [NO_3^-]^2}$$

and assuming that at steady state,  $J_{af} = J_o = J$

$$\begin{aligned} J_a \Delta_a + \frac{J_o \Delta_o}{K_{ex}[TBP]_{org}^2 [NO_3^-]^2} &= [UO_2^{2+}]_f \\ J \left( \frac{\Delta_a + \Delta_o}{K_{ex}[TBP]_{org}^2 [NO_3^-]^2} \right) &= [UO_2^{2+}]_f \quad (9) \\ J &= \frac{[UO_2^{2+}]_f}{\Delta_a + (\Delta_o / K_{ex}[TBP]_{org}^2 [NO_3^-]^2)} \\ J &= \frac{K_{ex}[TBP]_{org}^2 [NO_3^-]^2 [UO_2^{2+}]_f}{\Delta_o + \Delta_a K_{ex}[TBP]_{org}^2 [NO_3^-]^2} \quad (10) \end{aligned}$$

where  $\Delta_o = 1/k_m$  and  $\Delta_a = 1/k_i$  are organic and aqueous mass transfer resistances.

Taking into account that in membrane phase

$$[TBP]_{org}^0 = [TBP]_{org} + 2[U]_{org}$$



where  $[TBP]_{org}^0$  is the total concentration of extractant (TBP) and  $[TBP]_{org}$  is the free extractant concentration, for high metal concentrations

$$[TBP]_{org}^0 \cong 2[U]_{org} \quad (11)$$

substituting value of  $[U]_{org}$  from Eq. (11) into Eq. (7b)

$$[TBP]_{org}^2 = \frac{[TBP]_{org}^0}{2[UO_2^{++}][NO_3^-]^2 K_{ex}} \quad (12)$$

Substituting Eq. (12) into Eq. (10), we get,

$$J = \frac{(K_{ex}[TBP]_{org}^0[NO_3^-]_{aq}^2/2[UO_2^{++}][NO_3^-]_{aq}^2 K_{ex})[UO_2^{++}]_f}{\Delta_o + \Delta_a K_{ex}[TBP]_{org}^2[NO_3^-]_{aq}^2}$$

or

$$\begin{aligned} J &= \frac{[TBP]_{org}^0}{2\Delta_o + 2\Delta_a K_{ex}[TBP]_{org}^2[NO_3^-]_{aq}^2} \\ J &= \frac{[TBP]_{org}^0}{2\Delta_o + 2\Delta_a K_{ex}([TBP]_{org}^0[NO_3^-]^2/2[UO_2^{++}][NO_3^-]^2 K_{ex})} \\ &= \frac{[TBP]_{org}^0[UO_2^{++}]}{2\Delta_o[UO_2^{++}] + \Delta_a[TBP]_{org}^0} \end{aligned} \quad (13)$$

If in the last expression [Eq. (13)] the term  $\Delta_a ([TBP]_{org}^0)$  is neglected (because  $\Delta_a \ll \Delta_o$ ) and the diffusion is controlled in the organic phase, we obtain the following expression for metal flux:

$$J = \frac{[TBP]_{org}^0}{2\Delta_o} \quad (14)$$

Noting that by definition

$$J = -\frac{CV}{At}$$

If  $C = U$  and differentiating with respect to  $t$

$$J = -\frac{d[U]V}{dtA}$$



or

$$J \frac{A}{V} dt = -d[U]$$

$$d[U] = -J \frac{A}{V} dt$$

and integrating the flux equation with respect to time, we obtain the expression for the metal concentration

$$\int d[U] = -J \frac{A}{V} \int dt$$

From Eq. (14)

$$\begin{aligned} \int d[U] &= -\frac{[TBP]_{org}^0 A}{2\Delta_o V} \int dt \\ [U]_{in}^0 - [U]_{in} &= \frac{[TBP]_{org}^0 k_m A}{2V_f} t \end{aligned} \quad (15)$$

where  $[U]_{in} = \text{initial}$  and  $k_m = 1/\Delta_o$

Figure 5 plotted using Eq. (15) which show the kind of curve experimentally obtained when the initial metal concentration in the feed was  $5.0 \times 10^{-2} \text{ M}$  and the concentration of TBP in the membrane phase is  $1.09 \text{ M}$ . The slope of the straight line and Eq. (15) allow us to evaluate the membrane mass transfer coefficient ( $k_m$ ). The membrane diffusion coefficient ( $D_{eff}$ ) of  $\text{UO}_2(\text{NO}_3)_2 \cdot 2\text{TBP}$  when all the carrier is bound to the metal ions is evaluated as follows:

$$D_{eff} = k_m t_m \tau \quad (16)$$

where,  $D_{eff}$  is the diffusion coefficient,  $k_m$  is the membrane mass transfer coefficient,  $t_m$  is the thickness of the membrane, and  $\tau$  is the tortuosity. The calculated value of membrane mass transfer coefficient ( $k_m$ ) was  $4.08 \times 10^{-9} \text{ cm sec}^{-1}$  and  $D_{eff}$  was  $0.11 \times 10^{-9} \text{ cm}^2 \text{ sec}^{-1}$ , which is some what lesser than the value evaluated by Bobcock et al.,<sup>[24]</sup> e.g.,  $6 \times 10^{-9} \text{ cm}^2 \text{ sec}^{-1}$ , for the membrane diffusion coefficient of the complex formed between uranyl sulfate and tertiary amine Alamine 336 in the aromatic diluent Aromatic 150.

### Membrane's Stability and Reproducibility

For transport of trace metals, long term stability of the HFSLM is a key parameter. Plutonium transport and perconcentration measurements were made by operating the HFSLM system for 26 cycle (400 min) without



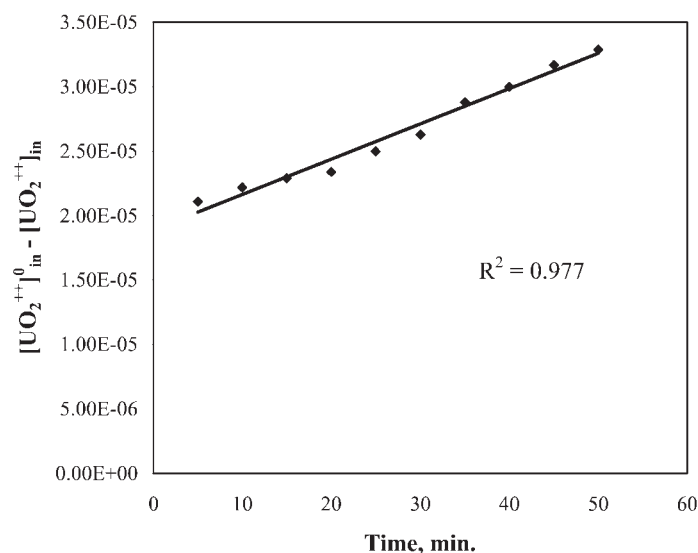


**Figure 5.**  $[UO_2^{++}]_{in}^0 - [UO_2^{++}]_{in}$  plotted vs. time ( $t$ ) for higher concentration of uranium using 1.09 M TBP as the carrier. Slope:  $3 \times 10^{-7} \text{ mol dm}^{-3}$ ; U(VI) in the feed:  $5.0 \times 10^{-2} \text{ mol dm}^{-3}$ .

re-impregnating the membrane. The stability of the membrane phase was checked by continuous run of impregnated module, and by checking intermixing of source phase to receiving phase. Figure. 6 shows that the permeability of the HFSLM was quite remarkable, during subsequent cycle of 400 min, no leaching of organic phase including leak was observed. This was confirmed by spiking of  $^{137}\text{Cs}$  in simulated source phase, at the end of 26 cycles maintaining the flow rate of  $3 \text{ mL min}^{-1}$  and no  $^{137}\text{Cs}$  was detected in the receiving phase. The permeability of Pu(IV) was measured and results from Fig. 7 shows that it was reproducible. No significant reduction in permeability was observed as carrier loss is insignificant and the device can be used for at least 400 min without re-impregnation.

Stability of the SLM depends on both the physical and chemical properties of the constituents. With a LM, extraction and stripping of metal occur on opposite sides of the membrane simultaneously. Hence carrier is being continuously regenerated. Thus a minimum of solvent inventory was required in these experiments—just the necessary amount to impregnate the pore structure of fibers.

In practice only few SLM systems are being applied in industrial scale, since the stability of the membranes is insufficient and, therefore, the lifetime of the membranes unpredictable. Little systematic research has been done to



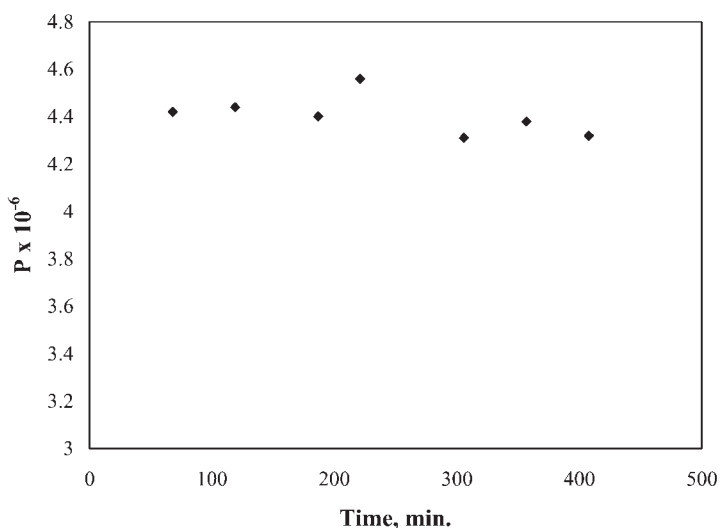


**Figure 6.** Stability of the HFSLM in recycle mode. Flow rate:  $3 \text{ mL min}^{-1}$ ; feed volume: 50 mL; Pu concentration in feed reservoir:  $2.08 \times 10^{-5} \text{ mol dm}^{-3}$ ; feed  $\text{H}^+$ : 3 M  $\text{HNO}_3$ ; carrier concentration: 1.09 M TBP.

find the causes of this instability. At the same time there is enough data on the consequences resulting from the instability problems. Causes of instability may vary from one system to another, but loss of the impregnating liquid (carrier or solvent) from the membrane to the source and strip solution is a major one. Two types of SLM instability effects can be distinguished. In the first place there is the problem of a decline in permeability as a function of time,<sup>[25,26]</sup> which is generally ascribed to the loss of carrier from the membrane phase.<sup>[27]</sup> In the second place a “break down” of the system can be observed, which means that a direct transport between the two phases is taking place.<sup>[28]</sup> The period of time after which such instability effects are observed can vary from some minutes to several months. This depends particularly on the type of solvent<sup>[28]</sup> and on the support used.<sup>[29,30]</sup> It is remarkable that in Ref.<sup>[30]</sup> the use of Accurel (microporous polypropylene from Enka) provides the most stable supported LMs. In addition to that the spongy opening of HF membrane's pores [Fig. 1(c) of Ref.<sup>[15]</sup>] offers more resistance to loss of organic content, which increases the life of HFSLM. The experimental results clearly indicated that the transport of Pu(IV) is held constant during the time period, which has been considered. For industrial application, the approach could be adopted for continuous re-impregnation mode as suggested by Chiarizia et al.<sup>[31]</sup>.



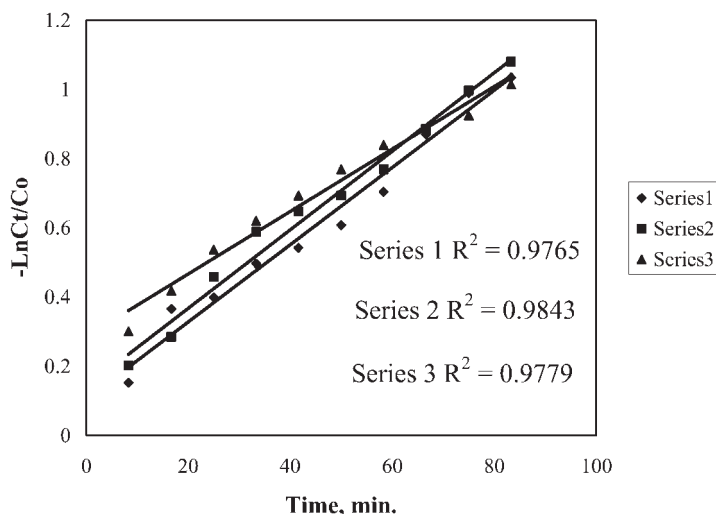


**Figure 7.** Plot of the reproducibility of HFSLM system. Carrier concentration: 1.09 M TBP in dodecane; strippant: 0.1 M  $\text{NH}_2\text{OH}\cdot\text{HCl}$  in 0.3 M  $\text{HNO}_3$ ; feed linear flow velocity:  $0.88 \text{ cm sec}^{-1}$ ; feed  $\text{H}^+$ : 3 M  $\text{HNO}_3$ ; effective surface area:  $33.91 \text{ cm}^2$ .

## CONCLUSIONS

The experimental results shows that the flux for U(VI) increases as the carrier concentration is increased up to 0.8 M; there after it remained constant and decreased after 30%, diffusion coefficient of Pu-TBP has decreased with increasing carrier concentration. Transport of metal ions greatly affected with agitated stage of strip solution. Larger surface area of membrane, gave more transport of metal ions. The graphical treatment of data by the slope analysis method gave us information about the diffusional resistance of metal ions–carrier complex. It was shown that the recovery/concentration of U(VI) and Pu(IV) from acidic medium selectively could be achieved through HFSLM.

## NOMENCLATURE

$C$	Metal concentration (M)
$V$	Volume ( $\text{cm}^3$ )
$A$	Effective surface area of the membrane [ $2\pi rNL$ ( $\text{cm}^2$ )]
$N$	Number of the fibers
$L$	Length of the fiber (cm)



$r$	Inner radius of the membrane
$D_{\text{eff}}$	Effective membrane diffusion coefficient of the Pu(IV)/U(VI) containing organic species ( $\text{cm}^2 \text{ sec}^{-1}$ )
$\Delta_a = d_a/D_a$	Transport resistance due to diffusion by the aqueous-feed boundary layer ( $\text{sec cm}^{-1}$ )
$\Delta_o = d_o/D_o$	Transport resistance due to diffusion through the membrane ( $\text{sec cm}^{-1}$ )
$k_m$	Membrane mass transfer coefficient ( $\text{cm sec}^{-1}$ )
$P$	Permeability coefficient ( $\text{cm sec}^{-1}$ )
$r_i$ and $r_o$	Inner and outer hollow fiber radius ( $\text{cm}^{-1}$ )
$d_a$	Thickness of the aqueous feed boundary layer (cm)
$d_o$	Thickness of membrane (cm)
$J_m$	Flux ( $\text{mol cm}^{-2} \text{ sec}^{-1}$ )
$t$	Time (sec)

### Subscripts

f and s	Refer to feed and stripping solution, respectively
i	For inner radii
o	For outer radii
M	Metal ion
aq	Aqueous
org	Organic
if	Interface

### Superscript

0	Concentration at time zero
$n$	Number

### Greek Letter

$\eta$	Viscosity
$\tau$	Tortosity

### REFERENCES

1. Kalachev, A.A.; Kardivarenko, L.M.; Plate, N.A.; Bargeev, V.V. Facilitated diffusion in immobilised liquid membranes-experimental verification of the jumping mechanism and percolation-threshold in membrane transport. *J. Membr. Sci.* **1992**, *75*, 1–5.



2. Frankenfeld, J.W.; Chan, R.P.; Li, N.N. Extraction of copper by liquid membranes. *Sep. Sci. Technol.* **1981**, *16* (4), 385–402.
3. Sastre, A.M.; Anil Kumar; Shukla, J.P.; Singh, R.K. Improved techniques in liquid membrane separation: an overview. *Sep. Purif. Methods* **1998**, *27*, 213–298.
4. Pickering, P.J.; Southern, C.R. Clean-up to chirality-liquid membranes as a facilitated technology? *J. Chem. Tech. and Bio. Technol.* **1997**, *68*, 417.
5. Werschulz, P. *New Membrane Technology in the Metal Finishing Industry, Toxic and Hazardous Waste*; Kugelman, I.J., Ed.; Technomic Publishing: Lancaster, PA, 1985; 444–454.
6. Shukla, J.P.; Anil Kumar; Singh, R.K.; Iyer, R.H. Separation of radiotoxic actinides from reprocessing wastes with liquid membranes. In *Chemical Separations with Liquid Membranes*; Bartsch, R.A., Way, J.D., Eds.; ACS Symp. Series, American Chemical Society: Washington, DC, 1996; 391–408, Chap. 27.
7. Anil Kumar; Sastre, A.M. Novel Membrane Based Process for Recovery of Gold from Cyanide Media Using Hollow Fiber Contactors: Impregnation and Non-Despersive Membrane Extraction Mode. Spanish Patent, 98 01736.
8. Anil Kumar; Sastre, A.M. Hollow fiber supported liquid membrane for the separation/concentration of gold(I) from aqueous cyanide media: modeling and mass transfer evaluation. *Ind. Eng. Chem. Res.* **2000**, *39*, 146–154.
9. Shukla, J.P.; Rathore, N.S.; Sonawane, J.V.; Sawant, S.R.; Venugopalan, A.K.; Singh, R.K.; Bajpai, D.D. DAE Symp. on Nuclear and Radiochemistry (NUCAR-99), B.A.R.C. Mumbai, Jan. 19–22, 1999.
10. Yang, M.C.; Cussler, E.L. Reaction dependent extraction of copper and nickel using hollow fibers. *J. Membr. Sci.* **2000**, *166*, 229–238.
11. Roberts, F.P. NUREG/CR-3584, Method 3, 1984.
12. Crouthamel, C.D.; Johnson, C.E. Spectrophotometric determination of uranium by thiocyanate method in acetone medium. *Anal. Chem.* **1952**, *24*, 1780.
13. Flaag, F. *Chemical Processing of Reactor Fuels*; John, F., Ed.; Flaag General Electric Company: Schenectady, New York, 1961; Academic Press: New York and London; 231.
14. Wick, O.J. *Plutonium Handbook, A Guide to the Technology*; New York, USA, 1967; Vol. 1, 464.
15. Rathore, N.S.; Sonawane, J.V.; Anil Kumar; Venugopalan, A.K.; Singh, R.K.; Bajpai, D.D.; Shukla, J.P. Hollow fiber supported liquid membrane: a novel technique for separation and recovery of plutonium from aqueous acidic wastes. *J. Membr. Sci.* **2001**, *189*, 119–128.



16. Reusch, C.F.; Cussler, E.L. Selective membrane transport. *AIChE J.* **1973**, *19*, 736–741.
17. Wickramasinghe, S.R.; Semmens, M.J.; Cussler, E.L. Hollow fiber modules made with hollow fiber fabric. *J. Membr. Sci.* **1993**, *84*, 1.
18. Lipnizki, F.; Field, R.W. Mass Transfer Performance for Hollow Fibre Modules with Shell-Side Axial Feed Flow: Using an Engineering Approach to Develop a Benchmark. *Proceedings of the International Congress on Membrane Science and Technology (ICOM'99)*, Toronto, June 1999.
19. Rathore, N.S.; Sonawane, J.V.; Anil Kumar; Venugopalan, A.K.; Singh, R.K.; Bajpai, D.D.; Shukla, J.P. DAE Symp. on Nuclear and Radiochemistry (NUCAR-2001), University of Pune, Feb. 7–11, 2001; 146.
20. Shukla, J.P.; Sonavane, J.V.; Kumar, A.; Singh, R.K. Amine – facilitated up-hill transport of plutonium (IV) cations across an immobilized liquid membrane. *Indian J. Chem. Technol.* **1996**, *3*, 145–148.
21. Danesi, P.R. A simplified model for the coupled transport of metal ions through hollow fiber supported liquid membranes. *J. Membr. Sci.* **1984**, *20*, 231–248.
22. Aamrani, F.Z.E.; Anil, K.; Beyer, L.; Florido, A.; Sastre, A.M. Mechanistic study of active transport of silver(I) using sulphur containing novel carriers across liquid membrane. *J. Membr. Sci.* **1999**, *152*, 263–275.
23. Urtiaga, A.M.; Ortiz, M.J.; Salzar, E.; Irabien, J.A. Supported liquid membranes for the separation-concentration of phenol. 1. Viability and mass-transfer evaluation. *Ind. Eng. Chem. Res.* **1992**, *31*, 877–886.
24. Bobcock, W.C.; Baker, R.W.; Lachapelle, E.D.; Smith, K.L. Coupled transport membranes. 3. The rate limiting steps in uranium transport with a tertiary amine. *J. Membr. Sci.* **1980b**, *7*, 89–100.
25. Teramoto, M.; Tanimoto, H. Mechanism of copper permeation through hollow-fiber liquid membrane. *Sep. Sci. Technol.* **1983**, *18*, 871–892.
26. Danesi, P.R. Separation of metal species by supported liquid membrane. *Sep. Sci. Technol.* **1984/1985**, *19* (11/12), 857–894.
27. Shimidzu, T.; Okushita, H. Carrier-mediated selective transport of  $Ga^{3+}$  from  $Ga^{3+}/Al^{3+}$  binary solution and  $Cu^{2+}$  from  $Cu^{2+}/Zn^{2+}$  binary solutions through alkylated cupferron-impregnated membrane. *J. Membr. Sci.* **1986**, *27*, 349–357.
28. Nakano, M.; Takahashi, K.; Tukeuchi, H. A method for continuous operation of supported liquid membranes. *J. Chem. Eng. Jpn.* **1987**, *20*, 326–328.
29. Muscatello, A.C.; Navratil, J.D.; Killion, M.E.; Price, M.Y. Supported extractant membranes for americium and plutonium recovery. *Sep. Sci. Technol.* **1987**, *22*, 843–854.



**Uranium and Plutonium Separation Using HFSLM**

**1319**

30. Tromp, M.; Burgard, M.; Leroy, M.J.F. Extraction of gold and silver cyanide complexes through supported liquid membranes containing macrocyclic extractant. *J. Membr. Sci.* **1988**, *38*, 295–300.
31. Chiarizia, R.; Horwitz, E.P.; Rickert, P.G.; Hodgson, K.M. Application of supported liquid membranes for removal of uranium from ground water. *Sep. Sci. and Technol.* **1990**, *25* (13–15), 1571–1586.

Received April 2003

Revised October 2003



## **Request Permission or Order Reprints Instantly!**

Interested in copying and sharing this article? In most cases, U.S. Copyright Law requires that you get permission from the article's rightsholder before using copyrighted content.

All information and materials found in this article, including but not limited to text, trademarks, patents, logos, graphics and images (the "Materials"), are the copyrighted works and other forms of intellectual property of Marcel Dekker, Inc., or its licensors. All rights not expressly granted are reserved.

Get permission to lawfully reproduce and distribute the Materials or order reprints quickly and painlessly. Simply click on the "Request Permission/Order Reprints" link below and follow the instructions. Visit the [U.S. Copyright Office](#) for information on Fair Use limitations of U.S. copyright law. Please refer to The Association of American Publishers' (AAP) website for guidelines on [Fair Use in the Classroom](#).

The Materials are for your personal use only and cannot be reformatted, reposted, resold or distributed by electronic means or otherwise without permission from Marcel Dekker, Inc. Marcel Dekker, Inc. grants you the limited right to display the Materials only on your personal computer or personal wireless device, and to copy and download single copies of such Materials provided that any copyright, trademark or other notice appearing on such Materials is also retained by, displayed, copied or downloaded as part of the Materials and is not removed or obscured, and provided you do not edit, modify, alter or enhance the Materials. Please refer to our [Website User Agreement](#) for more details.

### **Request Permission/Order Reprints**

Reprints of this article can also be ordered at

<http://www.dekker.com/servlet/product/DOI/101081SS120030484>